



Cite this: *Chem. Commun.*, 2023, 59, 10087

Received 22nd June 2023,  
Accepted 27th July 2023

DOI: 10.1039/d3cc03013j

rsc.li/chemcomm

# Development of regiodivergent asymmetric reductive coupling reactions of allenamides to access heteroatom-rich organic compounds

Stephen Collins and Joshua D. Sieber  \*

Organic compounds of biological importance often contain multiple stereogenic C-heteroatom functional groups (e.g. amines, alcohols, and ethers). As a result, synthetic methods to access such compounds in a reliable and stereoselective fashion are important. In this feature article, we present a strategy to enable the introduction of multiple C-heteroatom functional groups in a regiodivergent cross-coupling approach through the use of reductive coupling chemistry employing allenamides. Such processes allow for opportunities to access different heteroatom substitution patterns from the same starting materials.

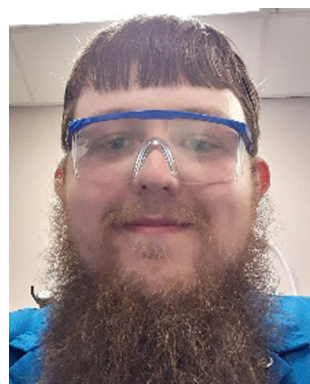
## Introduction

When considering organic architectures of important biological and medicinal activity, such compounds are often found to contain multiple heteroatom functional groups in a chiral arrangement (Fig. 1). As an example, the 1,2-aminoalcohol<sup>1,2</sup> motif alone is present in >300 000 compounds, >2000 natural products, and >80 Food and Drug Administration-approved drugs, according to a survey from 2019.<sup>3</sup> As a result, methodologies and synthetic strategies to enable efficient synthetic

access to these useful “heteroatom-rich” organic compounds is an important research endeavour.

In the context of identifying new tools to allow for the programmatic synthesis of diverse heteroatom-rich organic compounds, it can be argued that an ideal<sup>4,5</sup> strategic approach to access a functional group pair could arise through the use of a convergent<sup>6–8</sup> cross-coupling type process (Fig. 2). For example, catalytic coupling of two functionalized fragments *X* and *Y* enables access to a bis(functionalized) product through forging of the C–C bond (Fig. 2A). According to this design strategy, it is expected that the specific electronic nature of the functional groups present within *X* and *Y* (i.e. FG<sup>1</sup> and FG<sup>2</sup>) will dictate the type of cross-coupling reaction required to achieve the desired bond formation (Fig. 2B–D).<sup>9–11</sup> For instance, for a

Virginia Commonwealth University, Department of Chemistry 1001 West Main Street, Richmond, VA 23284, USA. E-mail: jdsieber@vcu.edu



Stephen Collins

Stephen Collins received his B.S. degree in chemistry from the University of North Carolina at Charlotte while working under Prof. Christopher Bejger. He is currently a PhD student in the Chemistry Department at the Virginia Commonwealth University. His doctoral studies are focused on asymmetric Cu-catalysed reductive coupling reactions utilizing allenamides to access chiral diamines and aminoalcohols.



Joshua D. Sieber

Joshua Sieber is an Assistant Professor in the Chemistry Department at the Virginia Commonwealth University since 2018. Prior to his academic appointment, he was a senior (2011 – 2016) and principal (2016 – 2018) scientist at Boehringer Ingelheim Pharmaceuticals, Inc. in the Chemical Development Process Chemistry Group. Having a background in complex organic molecule synthesis and asymmetric catalysis, his current research interests focus on developing catalytic asymmetric C–C bond forming reactions.



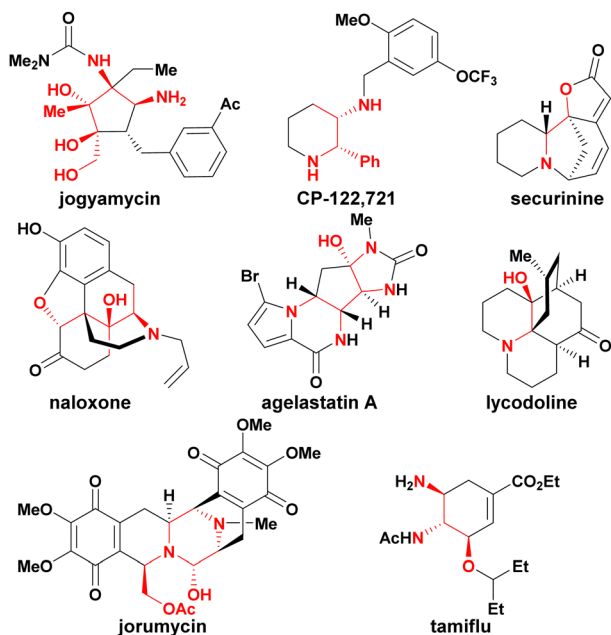


Fig. 1 Selected heteroatom-rich (*i.e.* N, O) natural products and bioactive organic compounds.

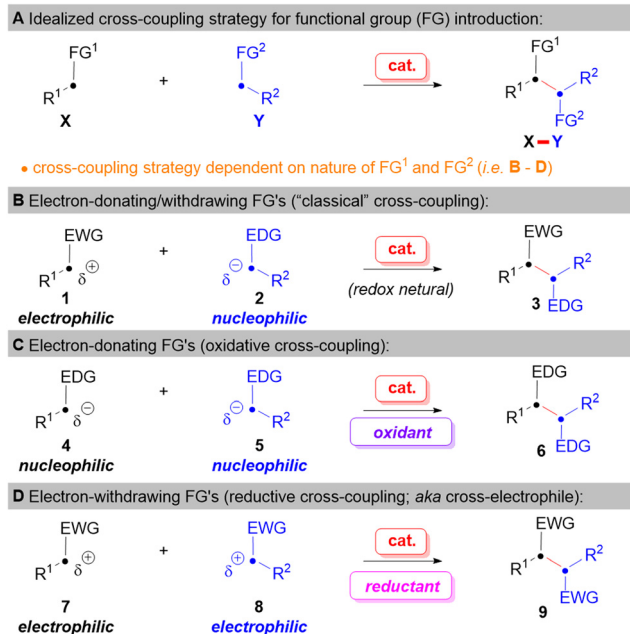


Fig. 2 Idealized strategy for the convergent integration of multiple functional groups through a convergent cross-coupling approach. EDG = electron-donating group, EWG = electron-withdrawing group.

case where one coupling fragment contains an electron-withdrawing functional group (EWG) and the other contains an electron-donating functional group (EDG), the carbon atoms attached to each functional group are polarized to be electrophilic and nucleophilic, respectively (Fig. 2B).<sup>9–11</sup> This scenario creates a common reactivity profile observed for two-electron chemical processes where each fragment contains a “matched”

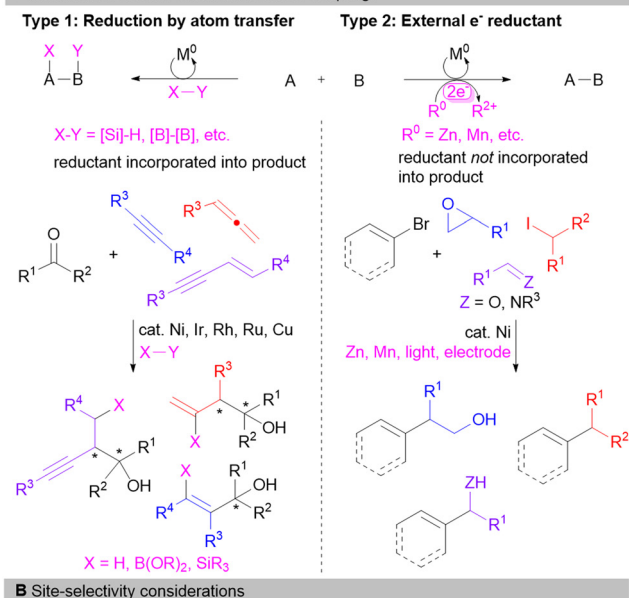
polarity profile leading to reagents that are poised to react with one another through a redox neutral process (electrophile/nucleophile pair). Classical cross-coupling processes<sup>12</sup> proceed by this type of redox neutral process (*e.g.* Suzuki–Miyaura,<sup>13</sup> Negishi,<sup>14</sup> Sonogashira,<sup>15</sup> *etc.*). However, for the case of fragments bearing two electron-donating functional groups (Fig. 2C: 4,5), these two nucleophilic fragments<sup>9,10</sup> result in an excess amount of electrons needed to forge the desired product **6**, and therefore, a stoichiometric oxidant is required to absorb the excess electrons in an oxidative coupling process.<sup>16,17</sup> In the last option, coupling partners that both contain electron-withdrawing functional groups (7,8; Fig. 2D), leads to a scenario whereby a deficiency of electrons needed to complete the desired coupling exists and as a result, a stoichiometric reductant is necessary in an overall reductive process.<sup>18,19</sup>

In relation to applying the cross-coupling approach outlined in Fig. 2 to the synthesis of *N*- and *O*-containing heteroatom-rich organic compounds (Fig. 1), a reductive coupling process would be needed considering the electron-withdrawing nature of *N*- and *O*-based substituents (Fig. 2D). Catalytic reductive coupling processes are known to occur through two types of mechanistic scenarios based on the nature of the reducing agent (Fig. 3A).<sup>18</sup> Pioneering work in the area of metal-catalysed reductive coupling began to emerge in the mid-late 1990's through the work of Mori,<sup>20</sup> Tamaru,<sup>21</sup> Montgomery,<sup>22</sup> Jamison,<sup>23</sup> Buchwald,<sup>24</sup> Kang,<sup>25</sup> and Kurosawa<sup>26</sup> through the Ni-catalysed coupling of unsaturated hydrocarbons with aldehydes<sup>27</sup> utilizing a terminal reductant to enable catalyst turnover through incorporation of atoms from the reductant into the final product (Type 1 process). Since that time, numerous researchers have developed powerful C–C bond forming processes based on this approach using a variety of different atom-transfer reductants (*e.g.* HSiR<sub>3</sub>, ZnR<sub>2</sub>, B<sub>2</sub>(OR)<sub>4</sub>, *etc.*).<sup>18,19</sup> In the late 2000s a resurgence in reductive coupling reaction development began for initially cross-electrophile sp<sup>2</sup>–sp<sup>3</sup> coupling reactions of aryl and alkyl halides by the groups of Lipshutz,<sup>28</sup> Wangelin,<sup>29,30</sup> Gong<sup>31</sup> and Weix.<sup>32,33</sup> These processes may proceed either by *in situ* formation of an organometallic nucleophile followed by a classical redox neutral coupling,<sup>34</sup> or in the case of Ni-catalysis, through a Type 2 reductive coupling process requiring electron-transfer from the reductant to the catalyst to enable catalyst turnover.<sup>33</sup> Such Type 2 techniques have been extended by a variety of researchers to other cross-electrophile couplings beyond aryl/alkyl sp<sup>2</sup>–sp<sup>3</sup> couplings with the requisite electrons provided from either stoichiometric transition metal reductants (*e.g.* Zn or Mn),<sup>35,36</sup> photocatalysis,<sup>37,38</sup> or electrochemically.<sup>39–42</sup>

It should be pointed out that an additional opportunity to the strategy outlined in Fig. 2D can be realized when considering the entire carbon framework of one of the coupling partners (*e.g.* **10**, Fig. 3B). For instance, in the simplified coupling to access **9**, only the 1,2-substituted product from C1-coupling is formed; however, in the case of **10**, if site-selective catalytic coupling with **7** could be realized through modification of the catalyst and reaction conditions, then a variety of heteroatom-substitution patterns (*i.e.* **11–13**) may be accessed from the



## A Mechanistic classes of reductive cross-coupling:



## B Site-selectivity considerations

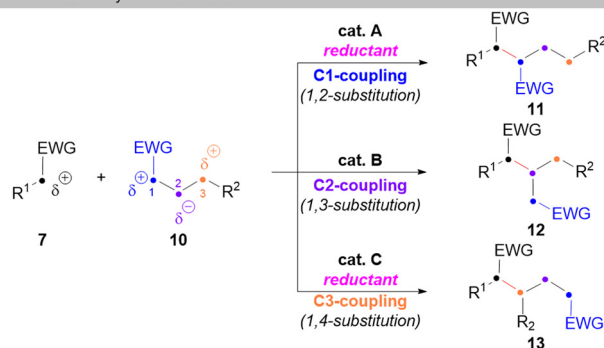


Fig. 3 Considerations for metal-catalysed reductive coupling as a tool for multiple heteroatom incorporation.

same starting materials. Along these lines, processes affording coupling at C1 and C3 of **10** would be required to be reductive in nature due to the chain polarization of **10** by the electron-withdrawing group, whereas coupling at C2 may be redox neutral. These electronic differences may be utilized to aid in the development of such site-selective, regiodivergent reaction processes.

The Sieber research group has been interested in developing methodologies for the asymmetric and regiodivergent reductive coupling of *N*- and *O*-substituted coupling partners according to the outlined strategy given in Fig. 3B as a tool for the synthesis of heteroatom-rich chiral organic compounds (Fig. 1).<sup>43–50</sup> As a result, we have primarily focused on accessing coupling products at C1 and C3 of the hypothetical starting material **10** (e.g. **11** and **13**, respectively) since these products are typically more challenging to access due to the dissonant charge affinity<sup>9–11</sup> produced by the relationship of the two electron-withdrawing heteroatom substituents.

To realize the outlined strategy of Fig. 3B, an appropriate reagent for **10** is necessary that can enable regiodivergent access to products such as **11** and **13**. We envisioned this could

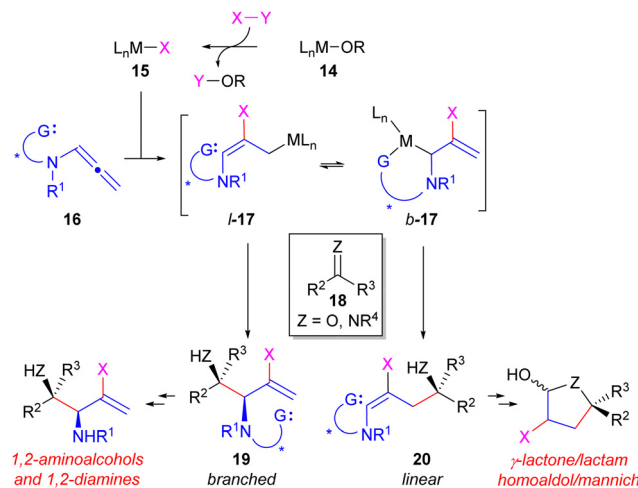


Fig. 4 Proposed reaction designs for multi-heteroatom functional groups.

be achieved using a *N*-substituted allene reagent (**16**, Fig. 4)<sup>51,52</sup> under a Type 1 reductive allylative process.<sup>53</sup> For instance, sigma-bond metathesis of a *M*-OR complex (**14**) with reductant *X*-*Y* followed by metalation of **16** may provide an equilibrating mixture of nucleophilic substituted allyl metal complexes *l*-**17** and *b*-**17**. Addition of these reagents to carbonyl or imine electrophiles (**18**) through chair-like transition states would provide access to either 1,2- (**19**) or 1,4-heteroatom (**20**) substituted products, respectively. Reductive allylation techniques incorporating a hydrogen atom from the reductant *X*-*Y* have been largely pioneered by the Krische group<sup>18</sup> utilizing allenes,<sup>54–57</sup> 1,3-dienes,<sup>58–60</sup> or enynes.<sup>61–63</sup> These powerful reactions represent atom economical alternatives to classical allylation processes utilizing preformed organometallic reagents and are typically catalysed by either Rh, Ir, or Ru. More recently, the Buchwald group<sup>64–68</sup> has developed orthogonal reductive allylation reactions under Cu-catalysis using silane as the terminal reductant. However, all these past precedented processes are typically branched-selective and access to the linear products are rare.<sup>43,47,69</sup> Furthermore, much of the work in this area has investigated the use of unsaturated hydrocarbon coupling partners bearing only carbon-substituents and the application and use of *N*-substituted reagents (e.g. **16**) has been less well developed prior to our work.<sup>3,54,70,71</sup>

In order to enable regiodivergency in reductive allylation reactions of **16**, our design strategy proposes incorporation of a tethered coordinating group 'G' in **16** as a technique to enable generation of the less common linear product **20** in these reactions. It was proposed that using a catalyst with a low coordination number (e.g. use of monodentate ligands) at the metal may facilitate formation of **20** through stabilization of *b*-**17** through internal coordination of the directing group 'G'. In contrast, use of a coordinatively saturated metal catalyst may in turn restore the more commonly observed branched-selectivity by inhibition of G-group binding to furnish **19**. As a result, access to highly valuable chiral 1,2-aminoalcohols and diamines or  $\gamma$ -lactones or lactams may be accessible from



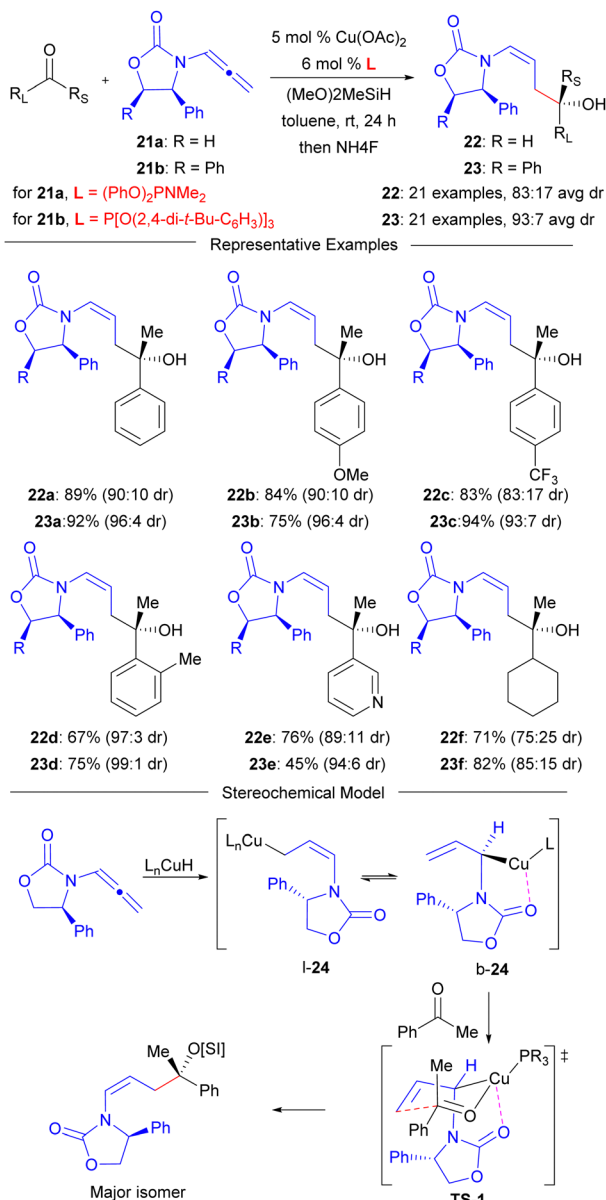
the same starting materials through selection of the reaction conditions. The development of these types of asymmetric strategies utilizing reagents **16** are summarized herein.

### Asymmetric auxiliary-controlled regiodivergent Cu-catalysed reductive coupling of allenamides and ketones

To realize the proposed strategy outlined in Fig. 4, an appropriate structure for **16** was required. Our group initially chose to investigate the use of the Evans-oxazolidinone derived allenamide **21a** (Scheme 1) for these processes that has been pioneered by the Hsung group<sup>51</sup> for other non-reductive coupling reactions due to the low cost of the Evans auxiliary.<sup>45</sup> Accordingly, the carbonyl group of the oxazolidinone must serve as the G-group of **16** to enable linear control. Furthermore, we chose

to study Cu-catalysed reductive coupling processes due to the improved sustainability and safety of Cu relative to the competitive Type 1 reductive coupling catalysts derived from the precious metals Ru, Rh, or Ir due to the high availability, low cost, and reduced toxicity of Cu compared with these other precious metal pre-catalysts.<sup>50</sup> Gratifyingly, a systematic study of monodentate phosphorous based ligands in the coupling of **21a** with ketone electrophiles demonstrated that high linear selectivity could be obtained to provide homoaldol products **22** in excellent yield and stereocontrol when using phosphoramidite ligand (PhO)<sub>2</sub>PNMe<sub>2</sub>.<sup>43</sup> The substrate scope in this process was shown to be quite broad, and an average stereocontrol of 83:17 dr could be obtained for the 21 examples investigated. A more detailed investigation<sup>47</sup> into factors controlling diastereoselectivity then led to the identification of an alternative system employing chiral allenamide **21b** with a readily available commercial aryl phosphite ligand to provide improved stereocontrol across the same 21 examples (93:7 avg. dr). Furthermore, empirical ligand studies supported the proposal that oxazolidinone coordination to Cu (e.g. **b-24**) enables linear control based on the observation that linear selectivity increased with decreasing ligand electron-donating ability (*i.e.* increasing Lewis acidity at Cu) and bidentate phosphine ligands led to a switch to branched selectivity.<sup>43,44</sup> Additionally, the observed product stereochemical outcome (*Z*-olefin geometry, alcohol absolute configuration) further supports oxazolidinone binding as an Evans chelate model<sup>72,73</sup> chair-like transition structure **TS-1** correctly rationalizes the observed stereochemistry.

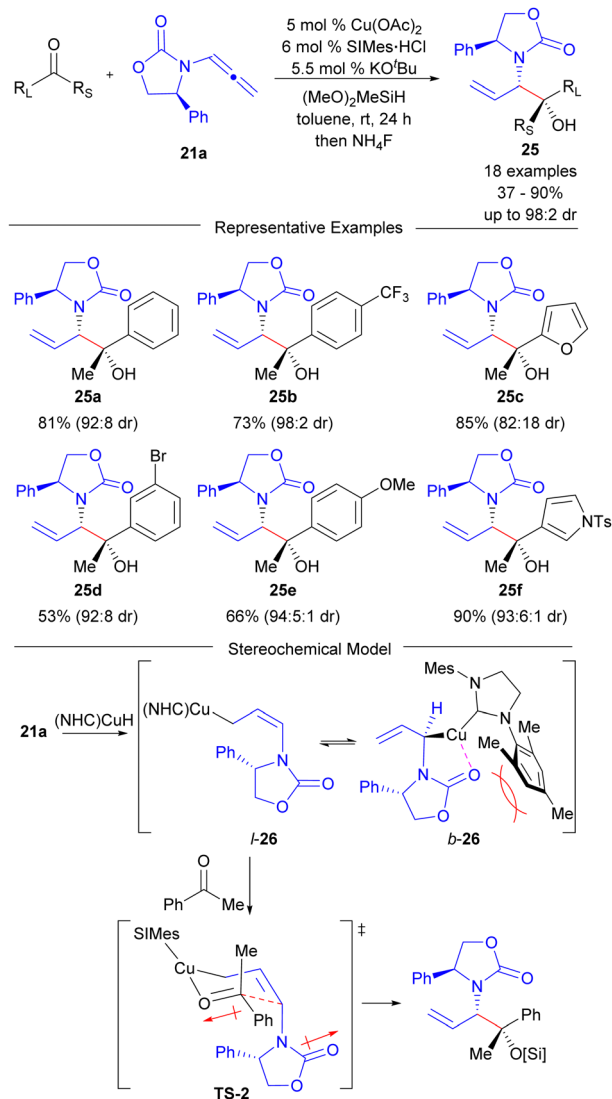
Upon obtaining confidence in our proposed design for regiocontrol, we next turned to developing a branched selective protocol through inhibition of oxazolidinone complexation to the Cu-catalyst.<sup>44</sup> While bidentate ligands were found to provide a turnover from linear to branched selectivity, ultimately use of the sterically hindered and highly electron-rich *N*-heterocyclic carbene (NHC) family of ligands proved optimal (Scheme 2). While this system was shown to be more sensitive to steric effects than the linear-selective system (Scheme 1), it was still able to produce branched products with good yields and high regio- and stereoselectivities. The ability of the NHC-based ligands to provide high branched regioselectivity is consistent with their well-known strong electron-donating<sup>74</sup> ability that may reduce the Lewis acidity at the Cu-catalyst to inhibit oxazolidinone binding. However, the steric effects induced at the metal catalyst by an NHC ligands is expected to be quite different relative to the cone-type effects of PR<sub>3</sub> type ligands measured by the cone angle.<sup>75</sup> Steric shielding of the Cu-catalyst towards oxazolidinone complexation by the mesityl-groups is also possibly responsible for the switch to branched selectivity. This possibility was corroborated by the observation that improved branched selectivity was observed when switching to the NHC ligand SIPr having a more sterically encumbered 2,6-diisopropylphenyl *N*-substituent on the NHC.<sup>44</sup> Finally, the observed major diastereomer produced in the reaction could be rationalized by an Evans dipole-minimization model (**TS-2**).<sup>72,76</sup>



**Scheme 1** Linear-selective reductive coupling of chiral oxazolidinone derived allenamides and ketones.

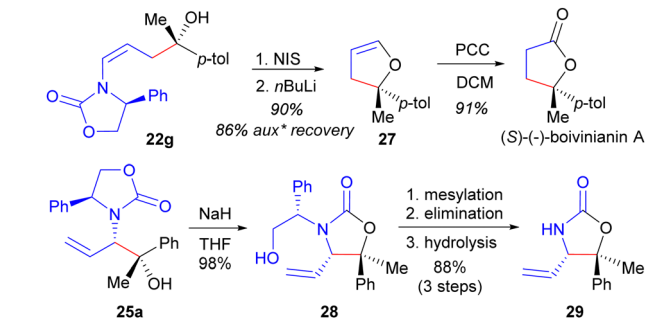




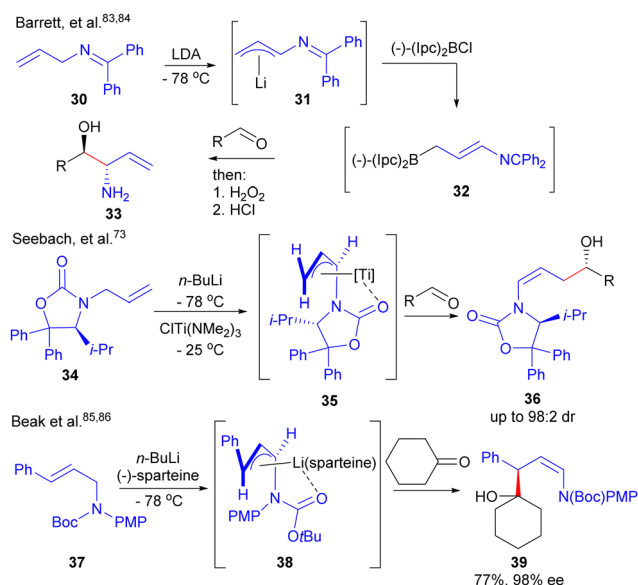


Scheme 2 Branched-selective reductive coupling of a chiral oxazolidinone derived allenamide and ketones.

The synthetic utility of the linear and branched reductive coupling products generated from the regiodivergent Cu-catalysed methodology was demonstrated through removal of the Evans oxazolidinone auxiliary (Scheme 3). Overall, the linear-selective reaction enables access to homoaldol synthons (22). Homoaldol derivatives are typically prepared through the generation of homoenolates,<sup>77,78</sup> and asymmetric variants are minimal.<sup>73,79,80</sup> Linear-product 22g underwent iodocyclization using NIS followed by an E1<sub>cb</sub>-elimination through Li-halogen exchange with *n*-BuLi to provide dihydrofuran 27 in excellent yield along with 86% recovery of the Evans oxazolidinone.<sup>47</sup> Dihydrofurans are useful synthetic intermediates that can be directly converted to  $\gamma$ -lactones through PCC oxidation<sup>81</sup> that enabled the synthesis of the natural product (S)-(-)-boivinianin<sup>82</sup> A. In regards to branched products 25, notably these were highly crystalline and could be enriched to single diastereomers 25 using crystallization from hexanes/ethyl acetate mixtures.<sup>44</sup>



Scheme 3 Auxiliary removal.



Scheme 4 Classical Aminoallylation Methods.

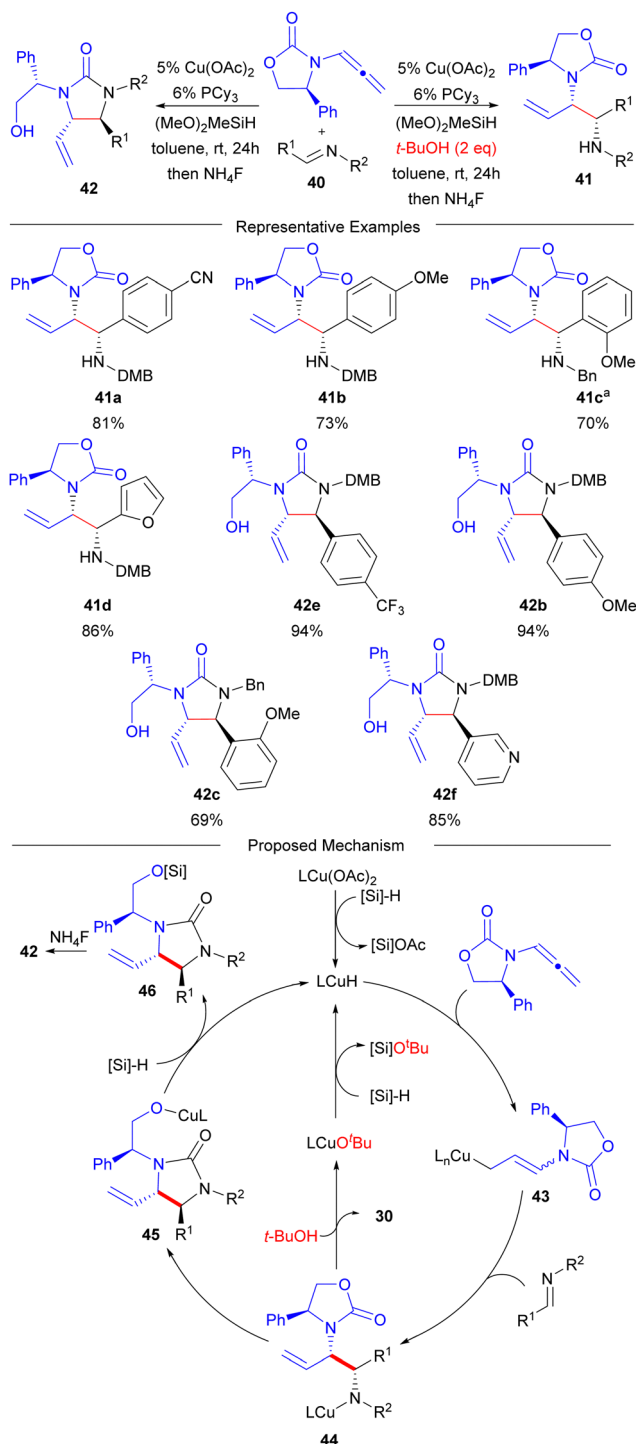
Base-induced carbonate migration allowed access to 28 whereby the phenethanol motif can be cleaved using a telescoped alcohol elimination process followed by enamide hydrolysis to produce 29 that can be hydrolysed to the 1,2-aminoalcohol if desired.

Overall, the methodologies outlined in Schemes 1 and 2 enable regiodivergent aminoallylation processes through generation of the reactive allylic organometallic nucleophile in a catalytic fashion under ambient conditions. Prior access to such compounds classically relied on generation of preformed organometallic nucleophiles from aza-allylanions (Scheme 4).<sup>73,83–86</sup> The paradigm shift in recent trends for carbonyl allylation employing allylmetal generation *in situ* by a metal catalyst has expanded functional group compatibility in these processes since strong bases and cryogenic temperatures are no longer required.

#### Asymmetric auxiliary-controlled Cu-catalysed reductive coupling of allenamides and imines: 1,2-diamine synthesis

After establishing the reductive coupling reactions utilizing ketone electrophiles, imines were next investigated as a protocol to access chiral 1,2-diamines (Scheme 5). Here, the





**Scheme 5** Branched-selective reductive coupling of a chiral oxazolidinone derived allenamide and imines.

monodentate electron-rich phosphine ligand  $\text{PCy}_3$  was identified as optimal, and it was discovered that this system could provide access to both chiral urea or diamine synthons depending on the introduction of *tert*-butanol as an additive.<sup>45</sup> The use of alcohol additives has been well established for  $\text{CuH}$  catalysed reductive coupling reactions.<sup>87,88</sup> Mechanistically, it was proposed that these followed a process similar to that involving

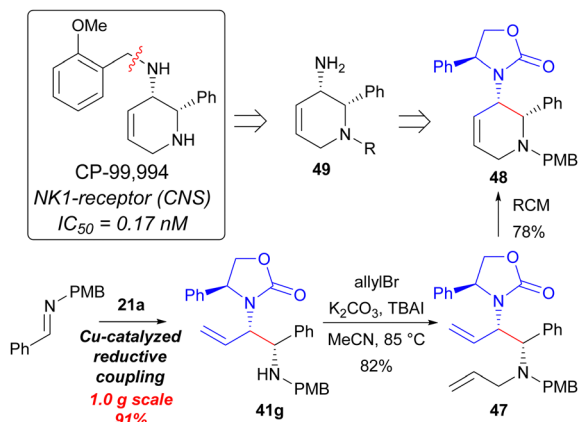
the branched 1,2-aminoalcohol, wherein linear allylcopper reagent 43 reacted with aldimine 40 through a chair-like transition structure to produce intermediate 44. In the ketone variant of these reactions (*vide infra*), the analogous *O*-intermediate of 44 would turnover through direct silylation; however, due to the weak bond strength of the  $\text{N-Si}$  bond,<sup>89</sup> there is no driving force for direct turnover through silylation of 44. As a result, in the absence of *tert*-butanol, intramolecular carbamate migration of 44 can occur to afford  $\text{Cu}$ -alkoxide intermediate 45 that can turnover through direct silylation leading to urea product 46. In contrast, in the presence of *t*-butanol, direct protonolysis of 44 can occur to generate copper alkoxide intermediate  $\text{L}_n\text{CuO}^t\text{Bu}$  that can regenerate the  $\text{CuH}$  catalyst by silylation with silane.

In the context of the substrate scope for the reaction with imine electrophiles, both electron-rich (40b,c) and electron-poor (40a,d,e,f) aryl aldimines participated well to afford the desired 1,2-diamine derivatives in high yields as single diastereomers.<sup>45</sup> Sterically hindered *ortho*-substituted aryl aldimines (40c) were also suitable coupling partners when the aldimine *N*-DMB protecting group was replaced with a less hindered *N*-benzyl group along with an increase in reaction temperature. Detailed density functional theory calculations on the reaction system were performed and revealed that stereo- and regiocontrol in the process was a result of Curtin-Hammett kinetics where a rapidly equilibrating mixture of *N*-substituted allylic  $\text{Cu}$  nucleophiles were present with the major product resulting from the lowest energy transition state for the addition of these rapidly equilibrating nucleophiles to the electrophilic imine through chair-like transition structures. Unfortunately, in regards to a regiodivergent process, the linear isomer of product was not observed under a variety of conditions tested. This is likely due to inhibition of the chair-like transition structure needed to access the linear product due to additional axial interactions between the  $\text{R}^2$ -group of the imine with the oxazolidinone that is not present when ketone electrophiles are used (*i.e.* TS-1, Scheme 1).

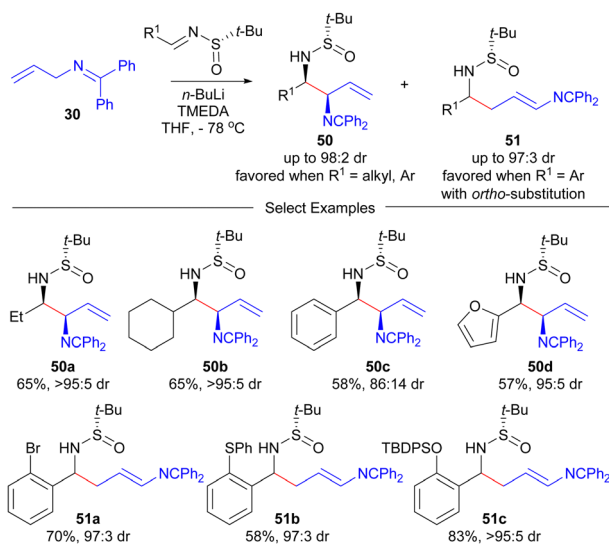
The potential synthetic utility of the imine reductive coupling methodology was applied to synthesis of 48 as a potential surrogate to the potent NK-1 inhibitor CP-99 994<sup>90</sup> (Scheme 6). The  $\text{Cu}$ -catalysed reductive coupling reaction was demonstrated on a 1.0 gram-scale on the benchtop using standard Schlenk techniques in excellent yield to provide 41g as a single diastereomer. Subsequent allylation of the PMB amine followed by ring-closing metathesis afforded 48.

The Prasad group<sup>91</sup> recently investigated the use of the azallyl anion produced by deprotonation of 30 with strong base in the addition reactions with Ellman's auxiliary<sup>92</sup> derived chiral sulfinyl imines (Scheme 7). The regiocontrol was determined to be dependent on the nature of the  $\text{R}^1$ -group of the sulfinyl imine. In general, branched products 50 were favoured, however, as the steric size of the  $\text{R}^1$ -group increases, the amount of linear product 51 increases. The highest yields of linear products 51 was obtained for *ortho*-substituted aryl  $\text{R}^1$ -groups. In general, excellent diastereoselectivities were obtained in these processes, but the identity of the major diastereomer of 51 was not determined.





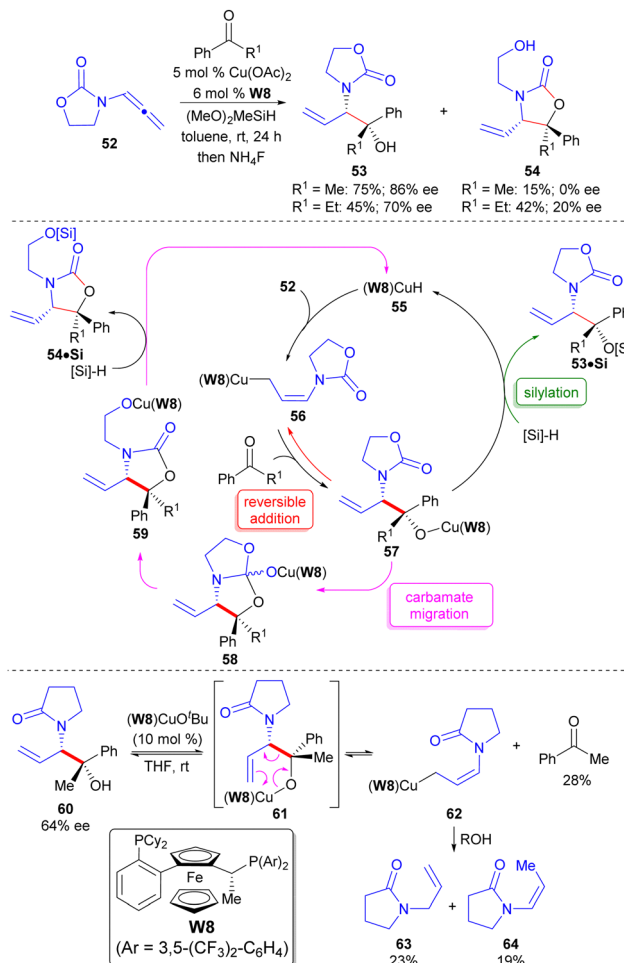
Scheme 6 Advancement to a cyclic diamine synthon.



Scheme 7 Prasad's aza-allyl anion based addition to Ellman's auxiliary derived sulfinyl imines.

### Enantioselective Cu-catalysed reductive coupling of allenamides and carbonyl-based electrophiles: 1,2-aminoalcohol synthesis

While the initial studies confirmed the ability to access alternate heteroatom substitution patterns from the same allenamide starting material through catalyst modulation,<sup>43,44,47</sup> stereocontrol was achieved by the chirality of the allenamide. It is reasonable to consider that an appropriately tuned chiral Cu-catalyst could enable the same type of transformations through enantioselective catalysis while utilizing an achiral allenamide. Such a strategy is attractive as the necessary chiral information can be used in sub-stoichiometric quantities. Towards this goal, initial investigations into the application of a simple achiral allenamide analogue to the past Evans' auxiliary derived system (*i.e.* 52) using chiral bis(phosphine) ligands to generate branched reaction product (53) led to the identification of Walphos-8 (**W8**) as optimal in reactions



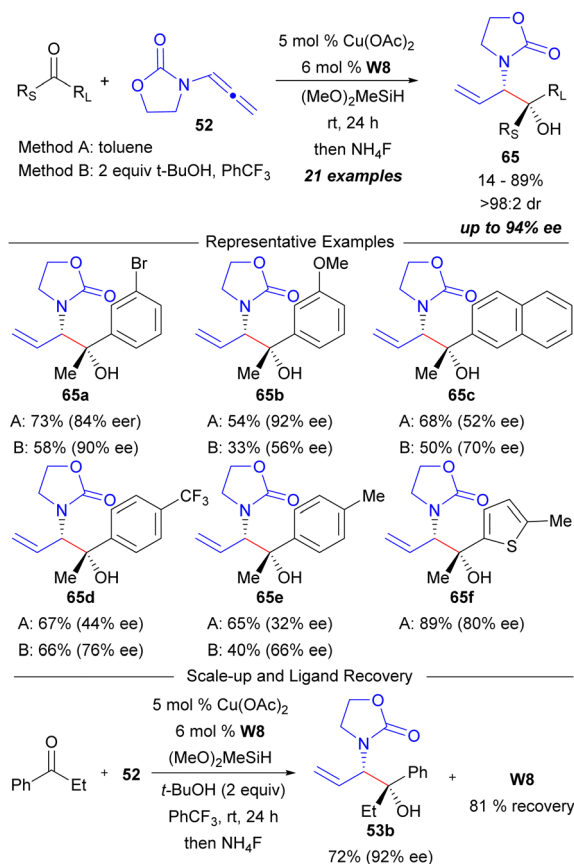
Scheme 8 Enantioselective reductive coupling of ketones and a cyclic allenamide to 1,2-aminoalcohol synthons.

utilizing aromatic ketones (Scheme 8).<sup>46</sup> Notably, it was observed that carbamate rearrangement product 54 was obtained as a side-product in these processes in variable amounts as a function of the nature of the  $R^1$ -alkyl group of the ketone. For instance, as the size of the  $R^1$ -group increased (*i.e.* Me to Et), the amount of rearrangement product 54 also increased. Furthermore, it was initially surprising to note that the enantiopurities of 53 and 54 were not identical. These results implied that a reversible allylcupration event ( $56 \rightarrow 57$ ) was occurring along with an on-cycle rearrangement process to 54 ( $57 \rightarrow 58 \rightarrow 59 \rightarrow 54\text{-Si}$ ). Because the intermediate stereoisomers of 57 do not need to convert to 54-Si at the same rate, epimerization of 57 can occur throughout the carbamate migration event due to the reversible allylcupration step. This competition in catalytic turnover events also rationalizes the effect of  $R^1$ -group on product distribution. As the  $R^1$ -group becomes larger, the rate of silylation of 57 (a bimolecular process) is decreased whereas the rate of carbamate rearrangement (a unimolecular process) is increased due to an enhanced Thorpe-Ingold effect<sup>93,94</sup> leading to increased amounts of rearranged product 54. Further support for the existence of a reversible allylcupration step was provided through reaction of 60, whose nitrogen was masked by a group



that could not undergo rearrangement, with a Walphos-8 derived Cu-alkoxide catalyst as a way to regenerate an analogue to intermediate **57** that may not rearrange (*i.e.* **61**). Retro-allylation<sup>95</sup> was observed to occur from this intermediate by observation of the formation of ketone (28%) and protonolysis products **63** and **64**. This is the first example of reversible allylation in metal-catalysed reductive coupling reactions.

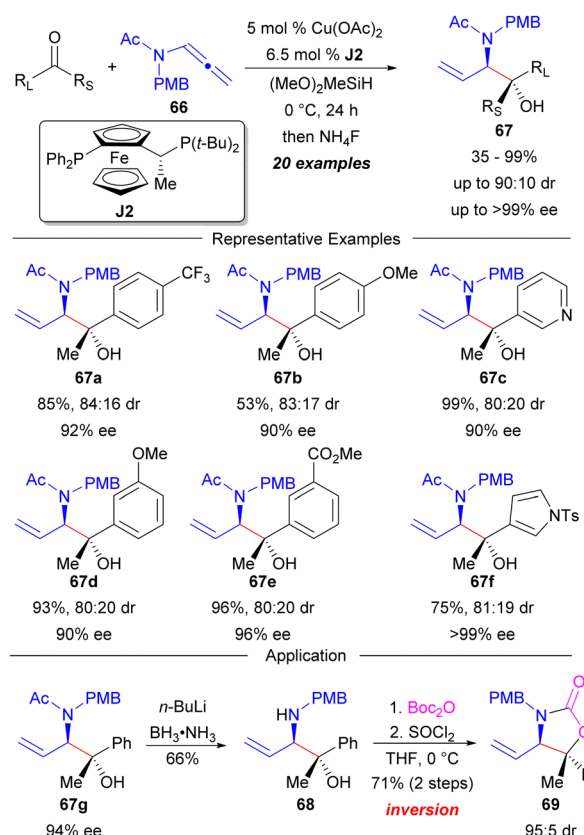
The overall reaction scope to access the *syn*-1,2-amino-alcohol synthons **53** was examined using the Walphos-8 derived Cu-catalyst system (Scheme 9).<sup>46</sup> Good yields with variable enantioselectivities were obtained for a variety of ketones when using a direct silylative turnover mechanism (Method A). The variable enantiocontrol was not surprising due to the determined on-cycle carbamate rearrangement problem (Scheme 8), and it was reasoned that additives that may facilitate the trapping of intermediate **57** may improve enantiocontrol. As such, the addition of *t*-butanol was developed under the idea that direct protonolysis of **57** may improve enantiocontrol (protonolysis turnover mechanism, Method B). In most cases, this resulted in an increase in enantiopurity but a decrease in yield was also obtained due to competitive protonation of the intermediate substituted allylic copper nucleophile (*i.e.* **56**). Notably, the ligand used in these processes can also be readily recovered which was demonstrated on a 1.0 mmol scale reaction.



**Scheme 9** Ketone scope in the (Walphos-8)Cu-catalysed reductive coupling of ketones and a cyclic allenamide.

Due to the variable enantioselectivities obtained when using cyclic carbamate derived allenamides that can undergo competitive on-cycle carbamate migration (*e.g.* **52**), it was hypothesized that substrate generality could be improved by using acyclic allenamides bearing substituents that could not undergo this problematic rearrangement (*e.g.* *N*-Ac, *N*-Bz, *etc.*). As a result, a second-generation system was investigated under this context and an optimal enantioselective system was identified when employing acyclic allenamide **66** in conjunction with a Josiphos-2 (**J2**) derived chiral Cu-catalyst (Scheme 10).<sup>48</sup> Notably, this new system was found to produce the opposite diastereomer in the reaction as compared to allenamide **52** (*anti*-selectivity obtained), and the yields and enantioselectivities for both electron-withdrawing and electron-donating substituted aryl ketones were high. Excellent results were also obtained for heterocycles (**67c,f**). Removal of the *N*-acetyl moiety of **67** could be achieved using lithium amidotrihydroborate (LAB) reduction<sup>96</sup> to furnish secondary amine **68** in a straightforward deprotection procedure. Gratifyingly, access to the overall *syn*-diastereomer could also be obtained through inversion of the oxygen-bearing carbon stereocenter of **68** by boc-protection of the amine followed by anchimeric-assisted internal substitution of the hydroxyl group utilizing SOCl<sub>2</sub> activation.<sup>97</sup>

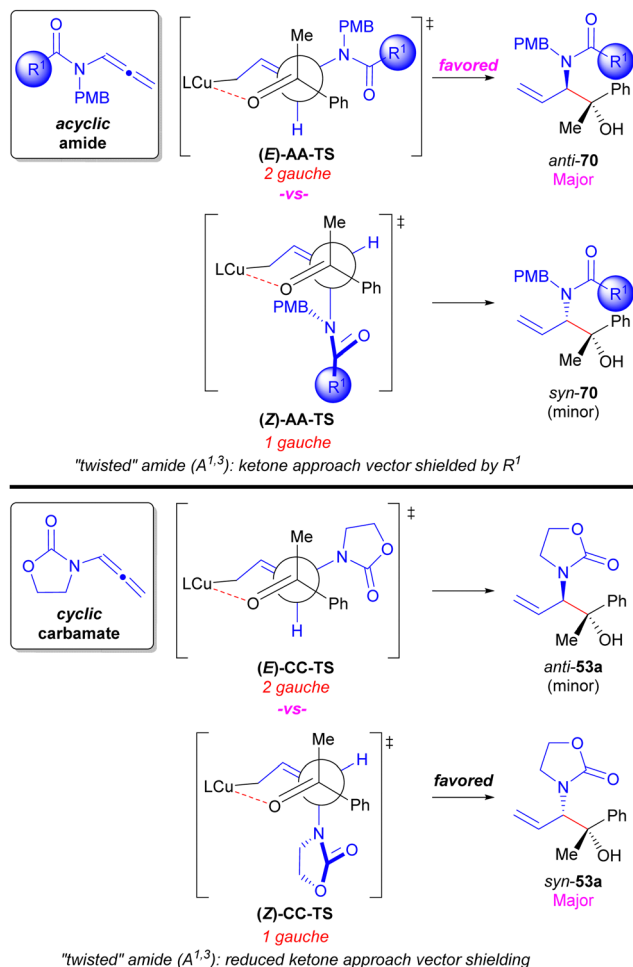
The diastereodivergency enabled through the nature of the *N*-substituents of the allenamide (*i.e.* acyclic *vs.* cyclic) could be rationalized considering chair-like transition state models



**Scheme 10** Improved enantiocontrol in the Cu-catalysed reductive coupling with ketones using an acyclic allenamide.







**Scheme 11** Diastereodivergency model for cyclic vs acyclic allenamides in Cu-catalysed asymmetric reductive coupling with ketone electrophiles.

depicted as their Newman projections in Scheme 11.<sup>48</sup> Stereo-control in Cu-catalysed reductive allylation reactions is typically a result of Curtin–Hammett kinetics for the addition of rapidly equilibrating substituted allylic copper nucleophilic intermediates to the electrophile.<sup>45,67</sup> As such, the *anti/syn* diastereo-control is a function of the olefin geometry of the *N*-substituted allylic intermediates with the *E*-enamide leading to *anti*-products (e.g. (*E*)-AA-TS and (*E*)-CC-TS) and the *Z*-enamide leading to *syn*-products (e.g. (*Z*)-AA-TS and (*Z*)-CC-TS). The preference of the reaction involving acyclic allenamides for the *anti*-diastereomer seems counterintuitive considering that the transition state leading to this product has two gauche interactions (i.e. (*E*)-AA-TS) compared to the one gauche interaction present in the transition state furnishing the *syn*-diastereomer (i.e. (*Z*)-AA-TS). However, when considering that *Z*-enamides are known to exist as "twisted" amides due to penalizing  $A^{1,3}$ -strain,<sup>98,99</sup> this twisting leads to steric shielding of the ketone approach vector by the  $R^1$ -group present in acyclic allenamides to destabilize (*Z*)-AA-TS and cause the *anti*-diastereomer of product to be favored. In contrast, the analogous *syn*-forming transition structure for cyclic allenamides (i.e. (*Z*)-CC-TS) has reduced steric shielding of the ketone

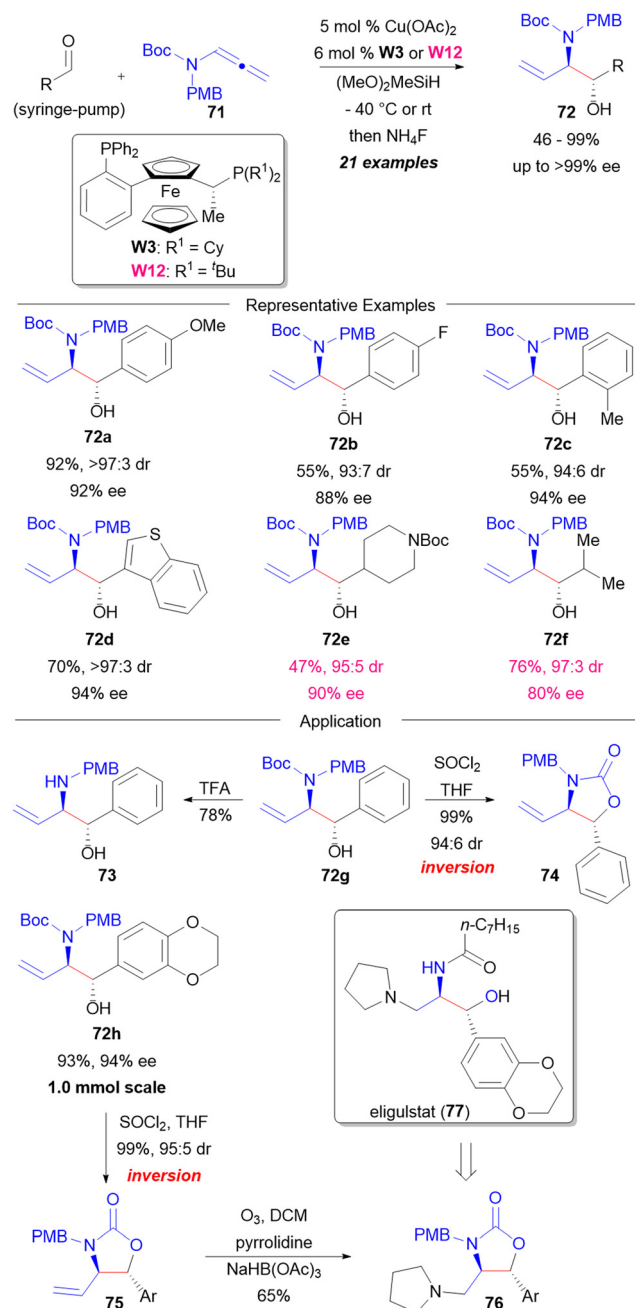
approach vector since the substituents are tied back in a ring and rotated away from the approaching ketone. This presumably allows for (*Z*)-CC-TS to be lower in energy to (*E*)-CC-TS that contains the larger number of gauche interactions affording overall *syn*-diastereoselectivity.

While Cu-catalysed reductive coupling reactions involving ketones produced aminoalcohols bearing tertiary alcohols, it is also desirable to expand the methodology towards generating those containing secondary alcohols by using aldehydes as coupling partners. Aldehydes are typically difficult coupling partners for CuH-catalysis due to competitive reduction of the aldehyde over hydrometalation of the unsaturated hydrocarbon coupling partner.<sup>64</sup> Of the rare examples of use of aldehydes in CuH-catalysis,<sup>68,100</sup> this can be circumvented by performing slow addition of the aldehyde to the reaction mixture. Utilizing this approach, a CuH-catalysed enantioselective reductive coupling of aldehydes and a *N*-Boc derived acyclic allenamide (**71**) was developed to provide access to chiral 1,2-aminoalcohols bearing a secondary alcohol motif (**72**, Scheme 12).<sup>50</sup> Again, the *anti*-diastereomer of product was the major diastereomer formed when using the acyclic allenamide **71**. The yields and enantioselectivities of this process ranged from good to excellent and both aromatic and aliphatic aldehydes could be used. Furthermore, the *N*-Boc group could be easily removed using TFA to access the free secondary amine of **73**. Notably, as with the previous acyclic allenamide/ketone coupling system, a *syn*-derivative (**74**) could also be accessed from the *anti*-products (e.g. **72g**) by anchimeric-assisted internal substitution of the secondary alcohol by the *N*-Boc group.<sup>97</sup> This invertive process was exploited in the context of studies towards the synthesis of eligulstat (**77**), an important compound for the treatment of Gaucher's disease.<sup>101</sup> Aminoalcohol precursor **72h** was prepared in high yield and enantioselectivity using the established reductive coupling process, followed by anchimeric-assisted cyclocarbamation to provide **75** having the requisite relative stereochemistry required for eligulstat. Subsequent ozonolysis of **75** followed by a reductive amination workup<sup>102</sup> with pyrrolidine afforded **76** as a potential precursor towards eligulstat.

The 1,2-aminoalcohol reaction products from aldehyde aminoallylation under Cu-catalysis (Scheme 12) have also been achieved utilizing Krische's hydrogen autotransfer<sup>18</sup> process initially in a non-enantioselective fashion employing Ru-catalysis,<sup>54,70,71</sup> and more recently in an enantioselective fashion<sup>3</sup> using Ir-catalysis (Scheme 13). By employing the *N*-phthaloyl derived allenimide **78**, chiral *anti*-1,2-aminoalcohol synthons can be accessed in excellent enantioselectivities.<sup>3</sup> Here the aldehyde coupling partner is employed at the alcohol oxidation state which is oxidized *in situ* through dehydrogenation by the catalyst to generate the necessary metal-hydride intermediate needed to hydrometalate the allene and provide the allylmatal nucleophile for addition to the formed aldehyde. Such hydrogen-borrowing processes are highly atom economical and attractive tools for complex molecule synthesis.

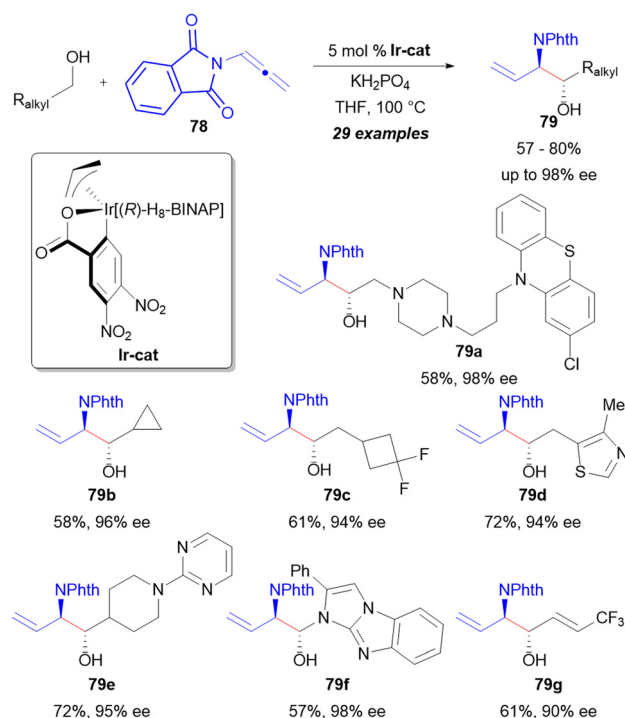
Besides the use of allenamides for the introduction of *N*-heteroatoms using reductive coupling, the Malcolmson group recently introduced the novel 2-azadiene<sup>103,104</sup> (**80**) and



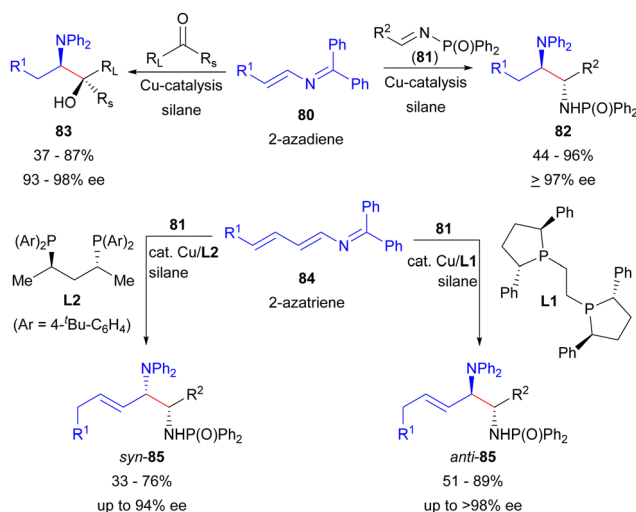


Scheme 12 Enantioselective Cu-catalysed reductive coupling of aldehydes with an acyclic allenamide.

2-azatriene<sup>105</sup> (84) reagents for the asymmetric synthesis of 1,2-aminoalcohols and 1,2-diamines by Cu-catalysed enantioselective reductive coupling (Scheme 14). While enantioselective coupling reactions with 2-azadienes (80) has been achieved with both ketone<sup>103</sup> and imine<sup>104</sup> electrophiles, saturated 1,2-aminoalcohols (83) or 1,2-diamines (82) are obtained. In contrast, the use of 2-azatrienes (84) provides access to unsaturated products 85 in reactions with imine<sup>105</sup> electrophiles (81). Notably, a diastereodivergent process could be



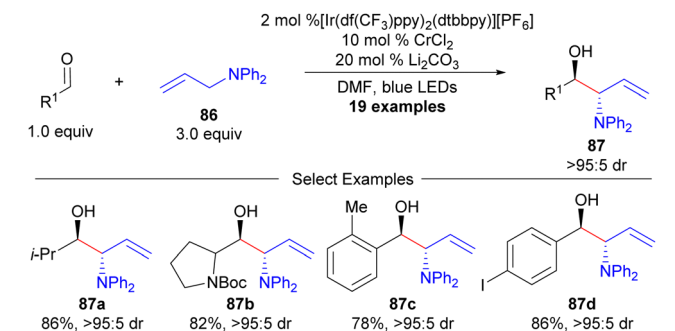
Scheme 13 Kricheldorf's enantioselective Ir-catalysed aminoallylation of aldehydes using hydrogen autotransfer with an allenamide.



Scheme 14 Malcolmson's enantioselective Cu-catalysed reductive coupling using 2-azadiene and 2-azatriene reagents.

developed employing 2-azatriene reagents 84 to afford either *anti*-85 or *syn*-85 by tuning the chiral ligand used for catalysis (L1 vs. L2, respectively). Furthermore, 2-azatriene reagents offer the possibility to access regioisomeric products according to the strategy outlined in Fig. 3B as a tool to prepare multiple different heteroatom substitution patterns, however, regio-divergent asymmetric processes employing 84 to exploit this potential have not yet been reported.





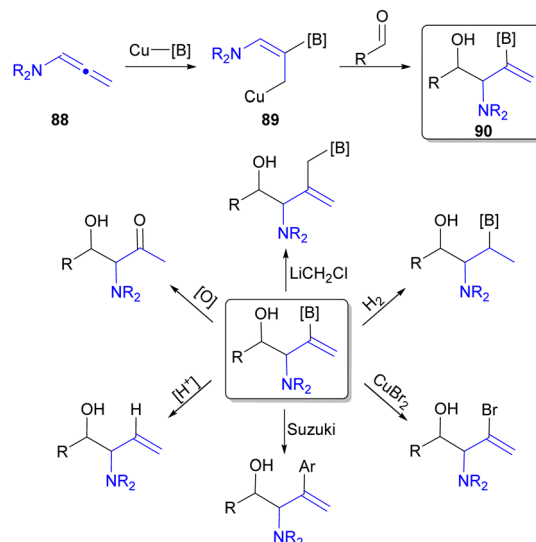
**Scheme 15** Glorius' redox neutral aminoallylation by dual photoredox and chromium catalysis.

Recently, photoredox catalysis has been utilized as a technique to enable Cr-catalysed allylation reactions by hydrogen atom abstraction (HAT, Scheme 15).<sup>106,107</sup> While this process is overall redox neutral, use of allylamine precursors (**86**) allows for branched-selective aldehyde aminoallylation in a non-enantioselective fashion.<sup>106</sup> While an enantioselective variant was achieved with allylsilanes (Hosomi-Sakurai reaction),<sup>107</sup> the enantioselective variant with a heteroatom-substituted allylic silane was not provided.

### Enantioselective reductive coupling of allenamides utilizing alternative reductants

All the previously discussed reductive coupling reactions employing *N*-substituted allenes utilized hydride based reducing agents to afford H-substituted products. However, reductive coupling can utilize alternative reductants to allow for the incorporation of additional functionality (Fig. 3A). For example, diboron reagents have been utilized in Type 1 reductive coupling processes<sup>108,109</sup> leading to products containing C–B functional group(s).<sup>18</sup> Accordingly, borylcupration<sup>110</sup> processes are well established, and therefore, utilizing diboronate reducing agents in place of silane for Cu-catalysed reductive coupling reaction of *N*-substituted allenes (**88**) can provide two main advantages over the use of silane reductants: (1) aldehyde reduction may be circumvented, and (2) addition of a C–B motif into the final product (e.g. **90**) that offers significant opportunities for further functionalization due to the vast diversity of transformations the C–B bond can undergo (Scheme 16).<sup>49</sup>

While borylative Cu-catalysed enantioselective reductive coupling reactions of carbon-substituted allenes using both aldehyde or imine electrophiles was initially reported by the groups of Hoveyda<sup>111</sup> and Procter,<sup>112</sup> respectively, reactions employing *N*-substituted allenes have been less developed<sup>113,114</sup> prior to our work.<sup>49</sup> Enantioselective Cu-catalysed borylative reductive coupling of allenimide **78** with aldehyde electrophiles was identified to proceed in high stereoselectivities using Ph-BPE (**L2**) as ligand to provide intermediate **91** (Scheme 17). This intermediate was found to be quite sensitive to protonolysis during silica gel chromatography, and therefore, further functionalization reactions of the C–B moiety were developed using telescoped processes through direct transformation of crude **91**. Protonolysis using AcOH led to products **92** from formal



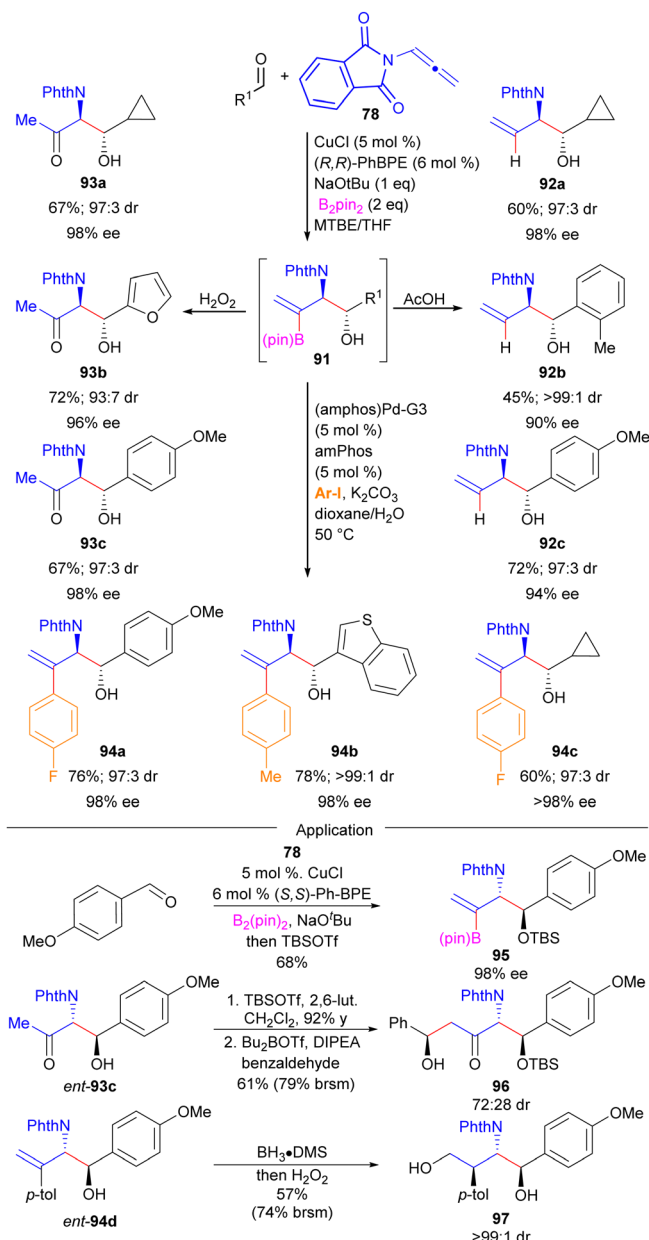
**Scheme 16** Synthetic opportunities available to Cu-catalysed reductive borylation of *N*-substituted allenes.

reductive coupling employing hydride reductants (e.g. **79**, Scheme 13). Oxidation of **91** using  $\text{H}_2\text{O}_2$  led to formal aldol products **93** whereas direct Suzuki–Miyaura cross coupling of **91** with aryl iodides or bromides allowed access to 1,1-disubstituted alkene compounds **94**.

The sensitivity of **91** to undergo protonolysis was hypothesized to result from the neighboring free hydroxyl group present.<sup>115</sup> Consequently, direct protection of the alcohol group as a TBS-ether through addition of TBSOTf to the completed reductive coupling reaction allowed for the isolation of intermediate **91** as the silyl ether (**95**). Additional transformations of the reaction products from the reductive borylation sequences were also demonstrated to enable access to heteroatom-rich compounds **96** and **97** from a *B*-aldol reaction or olefin hydroboration of *ent*-**93c** and *ent*-**94d**, respectively.

An additional interesting feature of the Cu-catalysed reductive borylation of allenimide **78** and aldehydes was the observed selective formation of the *anti*-diastereomer of product (**91**). Previous Cu-catalysed reductive borylation reactions of carbon-substituted allenes with aldehydes were demonstrated to afford the *syn*-diastereomer of product as the major isomer.<sup>111</sup> This typically is rationalized through addition of a substituted allylic copper nucleophile (*C*-**99**) to the aldehyde through a chair-like transition structure (*C*-**TS**, Scheme 18). Preference for the *Z*-alkene geometry of nucleophile *C*-**99** can be explained on steric grounds where the bulky (pin)B-moiety prefers a *trans*-relationship to the allene substituent ( $R_c$ ).<sup>111</sup> In contrast, the turnover in diastereoselectivity with *N*-phthaloyl derived allene **78** was rationalized through a catalyst directing effect by the *N*-phthaloyl group (*N*-**98**) to favour nucleophilic Cu-intermediate *N*-**99** having *E*-alkene geometry that may also benefit from carbonyl lone-pair donation into the vacant boron p-orbital.<sup>49</sup> Addition of *N*-**99** to aldehyde through *N*-**TS** leads to the observed *anti*-stereocontrol in reactions employing allene **78**. As a result, this demonstrates that not only can directing groups on the allene



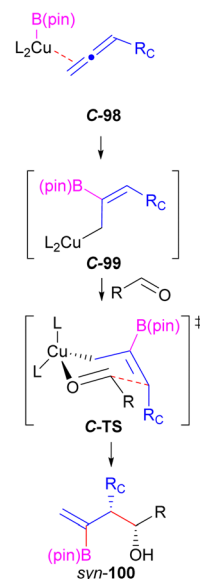


**Scheme 17** Cu-catalysed enantioselective reductive borylation of aldehydes with an *N*-phthaloyl allene.

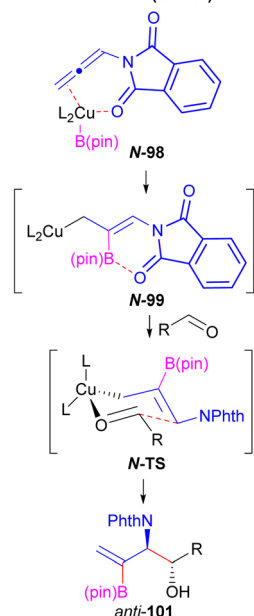
coupling partner be used to control regioselectivity (Fig. 3b, 4) but can also be used as a tool to impact stereocontrol.

In an alternative process developed by Chen,<sup>113</sup> access to similar products to **91** have also been obtained by a tandem Pt-catalyzed allene diboration/allylboration sequence (**103**, Scheme 19). While this pathway enables access to the *syn*-diastereomer of product, only racemates are obtained. Alternatively, Murakami<sup>114</sup> developed a strategy utilizing allylic transposition of vinyl diboronate **104** to **106** that can then be trapped *in situ* with aldehyde electrophiles to access *anti*-products **107** in a racemic fashion (Scheme 19). The opposite relative stereocontrol relative to Chen's process is a result of selective formation of the opposite alkene geometry (**106**) relative to

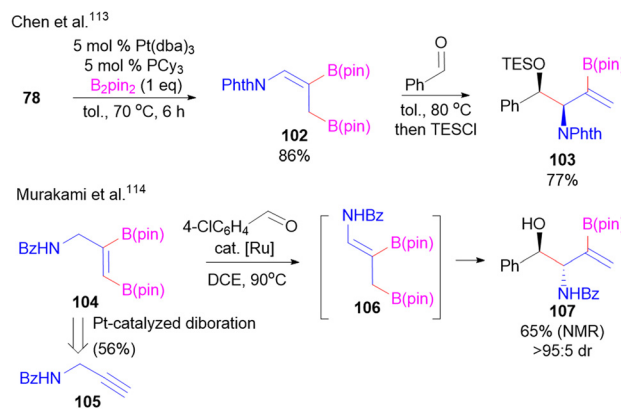
**C-substituted allene (Hoveyda):**



**N-substituted allene (Sieber):**



**Scheme 18** Diastereoselectivity differences between *C*- versus *N*-substituted allenes in Cu-catalysed reductive borylation.



**Scheme 19** Strategy towards racemic boryl-substituted 1,2-aminoalcohols through Pt-catalysed diboration/aldehyde allylboration.

**102** provided by the Ru-catalyst in the allylic transposition. The starting diboron reagent **104** used was previously prepared using Pt-catalysed diboration of alkyne **105**.<sup>116</sup>

## Conclusions

In this feature article, we demonstrate that the use of *N*-substituted allenes in asymmetric reductive coupling reactions represent a convenient tool towards enabling a synthetic strategy whereby multiple heteroatom substitution patterns can be generated using the same reaction starting materials. Accordingly, the use of an appropriate *N*-substituent to serve as a directing group and by catalyst modification allows for tuning of regiodivergency in these processes and can also lead to





differences in diastereoselection. Previous methods to access similar products typically required the use of strong bases and cryogenic reaction temperatures to generate preformed organometallic nucleophiles from aza-allyl anion equivalents. Modern reductive coupling processes allow for increased functional group compatibility and more convenient setup by operating under ambient conditions. Overall, the development of reductive coupling asymmetric processes of heteroatom-substituted unsaturated hydrocarbons are still relatively underdeveloped. For instance, only reactions of terminal allenamides have currently been reported, and investigation into alternative electrophile addition pathways, such as 1,4-conjugate addition when employing  $\alpha,\beta$ -unsaturated carbonyl compounds have not yet been disclosed. While both 1,2- and 1,4-heteroatom substitution has been demonstrated in these processes, significantly more methods are available for generation of 1,2-substituted products over the 1,4-substituted derivatives. Future work in this area is needed to enable additional processes and strategies to increase the types of heteroatom substitution patterns that can be accessed (e.g. 1,3-; 1,4-; 1,5-; 1,6-substitution, etc.), and expand the scope of the heteroatom-substituted unsaturated coupling partners employed (e.g. 1,1-disubstituted or chiral 1,3-disubstituted allenamides).

## Conflicts of interest

There are no conflicts to declare.

## Acknowledgements

The authors thank past and present group members for their significant contributions, as their names appear in cited references from our group. We acknowledge laboratory startup funding that has supported this work from the Virginia Commonwealth University and the Bill and Melinda Gates Foundation (Medicines for All Institute Grant, OPP#1176590). We also acknowledge the National Science Foundation (CHE-2143712) and REU supported students (CHE-1851916) for additional support that has contributed to this work. Solvias is acknowledged for the generous donation of **W12**.

## Notes and references

- 1 E. K. Davison and J. Sperry, *J. Nat. Prod.*, 2017, **80**, 3060–3079.
- 2 S. R. S. Saibabu Kotti, C. Timmons and G. Li, *Chem. Biol. Drug Des.*, 2006, **67**, 101–114.
- 3 K. Spielmann, M. Xiang, L. A. Schwartz and M. J. Krische, *J. Am. Chem. Soc.*, 2019, **141**, 14136–14141.
- 4 J. B. Hendrickson, *J. Am. Chem. Soc.*, 1975, **97**, 5784–5800.
- 5 T. Gaich and P. S. Baran, *J. Org. Chem.*, 2010, **75**, 4657–4673.
- 6 R. Dach, J. J. Song, F. Roschangar, W. Samstag and C. H. Senanayake, *Org. Process Res. Dev.*, 2012, **16**, 1697–1706.
- 7 D. Urabe, T. Asaba and M. Inoue, *Chem. Rev.*, 2015, **115**, 9207–9231.
- 8 Y. Gao and D. Ma, *Acc. Chem. Res.*, 2021, **54**, 569–582.
- 9 D. Seebach, *Angew. Chem., Int. Ed. Engl.*, 1979, **18**, 239–258.
- 10 D. A. Evans and G. C. Andrews, *Acc. Chem. Res.*, 1974, **7**, 147–155.
- 11 S. E. Dibrell, Y. Tao and S. E. Reisman, *Acc. Chem. Res.*, 2021, **54**, 1360–1373.
- 12 L. C. Campeau and N. Hazari, *Organometallics*, 2019, **38**, 3–35.
- 13 N. Miyaura, K. Yamada and A. Suzuki, *Tetrahedron Lett.*, 1979, **20**, 3437–3440.
- 14 E. Negishi, A. O. King and N. Okukado, *J. Org. Chem.*, 1977, **42**, 1821–1823.
- 15 K. Sonogashira, Y. Tohda and N. Hagihara, *Tetrahedron Lett.*, 1975, **50**, 4467–4470.
- 16 A. Lei, W. Shi, C. Liu and W. Liu, *Oxidative Cross-Coupling Reactions*, Wiley-VCH, Verlag GmbH & Co., 2016.
- 17 I. Funes-Ardoiz and F. Maseras, *ACS Catal.*, 2018, **8**, 1161–1172.
- 18 T. Agrawal and J. D. Sieber, *Synthesis*, 2020, 2623–2638.
- 19 M. Holmes, L. A. Schwartz and M. J. Krische, *Chem. Rev.*, 2018, **118**, 6026–6052.
- 20 Y. Sato, M. Takimoto, M. Mori, K. Hayashi, T. Katsuhara and K. Takagi, *J. Am. Chem. Soc.*, 1994, **116**, 9771–9772.
- 21 M. Kimura, A. Ezoe, K. Shibata and Y. Tamara, *J. Am. Chem. Soc.*, 1998, **120**, 4033–4034.
- 22 E. Oblinger and J. Montgomery, *J. Am. Chem. Soc.*, 1997, **119**, 9065–9066.
- 23 K. M. Miller, W. S. Huang and T. F. Jamison, *J. Am. Chem. Soc.*, 2003, **125**, 3442–3443.
- 24 N. M. Kablaoui and S. L. Buchwald, *J. Am. Chem. Soc.*, 1995, **117**, 6785–6786.
- 25 S. Kang and S. Yoon, *Chem. Commun.*, 2002, 2634–2635.
- 26 S. Ogoshi, M. A. Oka and H. Kurosawa, *J. Am. Chem. Soc.*, 2004, **126**, 11802–11803.
- 27 J. Montgomery, *Angew. Chem., Int. Ed.*, 2004, **43**, 3890–3908.
- 28 A. Krasovskiy, C. Duplais and B. H. Lipshutz, *J. Am. Chem. Soc.*, 2009, **131**, 15592–15593.
- 29 W. M. Czaplik, M. Mayer and A. J. Von Wangelin, *Angew. Chem., Int. Ed.*, 2009, **48**, 607–610.
- 30 W. M. Czaplik, M. Mayer, S. Grupe and A. J. Von Wangelin, *Pure Appl. Chem.*, 2010, **82**, 1545–1553.
- 31 X. Yu, T. Yang, S. Wang, H. Xu and H. Gong, *Org. Lett.*, 2011, **13**, 2138–2141.
- 32 D. A. Everson, R. Shrestha and D. J. Weix, *J. Am. Chem. Soc.*, 2010, **132**, 920–921.
- 33 D. A. Everson and D. J. Weix, *J. Org. Chem.*, 2014, **79**, 4793–4798.
- 34 C. E. I. Knappke, S. Grupe, D. Gärtner, M. Corpet, C. Gosmini and A. Jacobi Von Wangelin, *Chem. – Eur. J.*, 2014, **20**, 6828–6842.
- 35 X. Wang, Y. Dai and H. Gong, *Top. Curr. Chem.*, 2016, **374**, 1–29.
- 36 E. Richmond and J. Moran, *Synthesis*, 2018, 499–513.
- 37 R. T. Smith, X. Zhang, J. A. Rincón, J. Agejas, C. Mateos, M. Barberis, S. García-Cerrada, O. De Frutos and D. W. C. Macmillan, *J. Am. Chem. Soc.*, 2018, **140**, 17433–17438.
- 38 H. A. Sakai, W. Liu, C. Le and D. W. C. MacMillan, *J. Am. Chem. Soc.*, 2020, **142**, 11691–11697.
- 39 A. Jutand, *Chem. Rev.*, 2008, **108**, 2300–2347.
- 40 R. J. Perkins, D. J. Pedro and E. C. Hansen, *Org. Lett.*, 2017, **19**, 3755–3758.
- 41 R. J. Perkins, A. J. Hughes, D. J. Weix and E. C. Hansen, *Org. Process Res. Dev.*, 2019, **23**, 1746–1751.
- 42 T. J. Delano and S. E. Reisman, *ACS Catal.*, 2019, **9**, 6751–6754.
- 43 R. K. Blake, S. L. Gargaro, S. L. Gentry, S. O. Elele and J. D. Sieber, *Org. Lett.*, 2019, **21**, 7992–7998.
- 44 S. L. Gargaro, R. K. Blake, K. L. Burns, S. O. Elele, S. L. Gentry and J. D. Sieber, *Org. Lett.*, 2019, **21**, 9753–9758.
- 45 T. Agrawal, R. T. Martin, S. Collins, Z. Wilhelm, M. D. Edwards, O. Gutierrez and J. D. Sieber, *J. Org. Chem.*, 2021, **86**, 5026–5046.
- 46 R. K. Blake, M. D. Edwards and J. D. Sieber, *Org. Lett.*, 2021, **23**, 6444–6449.
- 47 D. B. Ho, S. Gargaro, R. K. Blake and J. D. Sieber, *J. Org. Chem.*, 2022, **87**, 2142–2153.
- 48 S. Collins and J. D. Sieber, *Org. Lett.*, 2023, **25**, 1425–1430.
- 49 S. L. Gargaro, R. K. Blake and J. D. Sieber, *Org. Lett.*, 2023, **25**, 4644–4649.
- 50 R. K. Blake and J. D. Sieber, *Org. Lett.*, 2023, **25**, 4730–4734.
- 51 T. Lu, Z. Lu, Z.-X. Ma, Y. Zhang and R. P. Hsung, *Chem. Rev.*, 2013, **113**, 4862–4904.
- 52 B. Alcaide and P. Almendros, *Adv. Synth. Catal.*, 2011, **353**, 2561–2576.
- 53 R. Blicke, M. Taillefer and F. Monnier, *Chem. Rev.*, 2020, **120**, 13545–13598.
- 54 E. Skucas, J. R. Zbieg and M. J. Krische, *J. Am. Chem. Soc.*, 2009, 5054–5055.



- 55 L. A. Schwartz, M. Holmes, G. A. Brito, T. P. Gonçalves, J. Richardson, J. C. Ruble, K. W. Huang and M. J. Krische, *J. Am. Chem. Soc.*, 2019, **141**, 2087–2096.
- 56 S. W. Kim, C. C. Meyer, B. K. Mai, P. Liu and M. J. Krische, *ACS Catal.*, 2019, **9**, 9158–9163.
- 57 M. Xiang, D. E. Pfaffinger, E. Ortiz, G. A. Brito and M. J. Krische, *J. Am. Chem. Soc.*, 2021, **143**, 8849–8854.
- 58 J. R. Zbieg, J. Moran and M. J. Krische, *J. Am. Chem. Soc.*, 2011, **133**, 10582–10586.
- 59 E. L. McInturff, E. Yamaguchi and M. J. Krische, *J. Am. Chem. Soc.*, 2012, **134**, 20628–20631.
- 60 K. D. Nguyen, D. Herkommer and M. J. Krische, *J. Am. Chem. Soc.*, 2016, **138**, 14210–14213.
- 61 L. M. Geary, S. K. Woo, J. C. Leung and M. J. Krische, *Angew. Chem., Int. Ed.*, 2012, **51**, 2972–2976.
- 62 L. M. Geary, J. C. Leung and M. J. Krische, *Chem. – Eur. J.*, 2012, **18**, 16823–16827.
- 63 K. D. Nguyen, D. Herkommer and M. J. Krische, *J. Am. Chem. Soc.*, 2016, **138**, 5238–5241.
- 64 Y. Yang, I. B. Perry, G. Lu, P. Liu and S. L. Buchwald, *Science*, 2016, **353**, 144–150.
- 65 E. Y. Tsai, R. Y. Liu, Y. Yang and S. L. Buchwald, *J. Am. Chem. Soc.*, 2018, **140**, 2007–2011.
- 66 R. Y. Liu, Y. Zhou, Y. Yang and S. L. Buchwald, *J. Am. Chem. Soc.*, 2019, **141**, 2251–2256.
- 67 C. Li, R. Y. Liu, L. T. Jesikiewicz, Y. Yang, P. Liu and S. L. Buchwald, *J. Am. Chem. Soc.*, 2019, **141**, 5062–5070.
- 68 C. Li, K. Shin, R. Y. Liu and S. L. Buchwald, *Angew. Chem., Int. Ed.*, 2019, **58**, 17074–17080.
- 69 H. Iwamoto, Y. Hayashi, Y. Ozawa and H. Ito, *ACS Catal.*, 2020, **10**, 2471–2476.
- 70 J. R. Zbieg, E. L. McInturff and M. J. Krische, *Org. Lett.*, 2010, **12**, 2514–2516.
- 71 W. Zhang, W. Chen, H. Xiao and M. J. Krische, *Org. Lett.*, 2017, **19**, 4876–4879.
- 72 M. Nerz-stormes and E. R. Thornton, *J. Org. Chem.*, 1991, **56**, 2489–2498.
- 73 C. Gaul and D. Seebach, *Helv. Chim. Acta*, 2002, **85**, 963–978.
- 74 R. Dorta, N. M. Scott, C. Costabile, L. Cavallo, C. D. Hoff and S. P. Nolan, *J. Am. Chem. Soc.*, 2005, **127**, 2485–2495.
- 75 C. A. Tolman, *Chem. Rev.*, 1977, **77**, 313–348.
- 76 D. A. Evans, J. M. Takacs, L. R. McGee, M. D. Ennis, D. J. Mathre and J. Bartroli, *Pure Appl. Chem.*, 1981, **53**, 1109–1127.
- 77 D. Hoppe, *Angew. Chem., Int. Ed. Engl.*, 1984, **23**, 932–948.
- 78 J. Y. Kang and B. T. Connell, *J. Am. Chem. Soc.*, 2010, **132**, 7826–7827.
- 79 D. Hoppe and O. Zschage, *Angew. Chem., Int. Ed. Engl.*, 1989, **28**, 69–71.
- 80 E. D. Burke, N. K. Lim and J. L. Gleason, *Synlett*, 2003, 390–392.
- 81 G. Piancatelli, A. Scettri and M. D'Auria, *Tetrahedron Lett.*, 1977, **18**, 3483–3484.
- 82 D. A. Mulholland, K. McFarland and M. Randrianarivelojosia, *Biochem. Syst. Ecol.*, 2006, **34**, 365–369.
- 83 A. G. M. Barrett, M. A. Seefeld and D. J. Williams, *J. Chem. Soc., Chem. Commun.*, 1994, 1053–1054.
- 84 A. G. M. Barrett, M. A. Seefeld, A. J. P. White and D. J. Williams, *J. Org. Chem.*, 1996, **61**, 2677–2685.
- 85 G. A. Weisenburger and P. Beak, *J. Am. Chem. Soc.*, 1996, **118**, 12218–12219.
- 86 D. J. Pippel, G. A. Weisenburger, N. C. Faibish and P. Beak, *J. Am. Chem. Soc.*, 2001, **123**, 4919–4927.
- 87 E. Ascic and S. L. Buchwald, *J. Am. Chem. Soc.*, 2015, **137**, 4666–4669.
- 88 R. Y. Liu, Y. Yang and S. L. Buchwald, *Angew. Chem., Int. Ed.*, 2016, **55**, 14077–14080.
- 89 T. L. Cottrell, *The Strength of Chemical Bonds*, 2nd edn, 1958.
- 90 M. C. Desai, S. L. Lefkowitz, P. F. Thadeio, K. P. Longo and R. M. Snider, *J. Med. Chem.*, 1992, **35**, 4911–4913.
- 91 M. B. Uphade, A. A. Reddy, S. P. Khandare and K. R. Prasad, *Org. Lett.*, 2019, **21**, 9109–9113.
- 92 M. T. Robak, M. A. Herbage and J. A. Ellman, *Chem. Rev.*, 2010, **110**, 3600–3740.
- 93 R. M. Beesley, C. K. Ingold and J. F. Thorpe, *J. Chem. Soc., Trans.*, 1915, **107**, 1080–1106.
- 94 B. L. Shaw, *J. Am. Chem. Soc.*, 1975, **97**, 3856–3857.
- 95 K. Nogi and H. Yorimitsu, *Chem. Rev.*, 2021, **121**, 345–364.
- 96 A. G. Myers, B. H. Yang and D. J. Kopecky, *Tetrahedron Lett.*, 1996, **37**, 3623–3626.
- 97 S. Kano, Y. Yuasa, T. Yokomatsu and S. Shibuya, *Heterocycles*, 1988, **27**, 1241–1248.
- 98 Z. Song, T. Lu, R. P. Hsung, Z. F. Al-Rashid, C. Ko and Y. Tang, *Angew. Chem.*, 2007, **119**, 4147–4150.
- 99 A. J. Clark, D. P. Curran, D. J. Fox, F. Ghelfi, C. S. Guy, B. Hay, N. James, J. M. Phillips, F. Roncaglia, P. B. Sellars, P. Wilson and H. Zhang, *J. Org. Chem.*, 2016, **81**, 5547–5565.
- 100 W. J. Jang and J. Yun, *Angew. Chem., Int. Ed.*, 2018, **57**, 12116–12120.
- 101 L. J. Scott, *Drugs*, 2015, **75**, 1669–1678.
- 102 H. Yung-Son and L. Ling, *Tetrahedron Lett.*, 1993, **34**, 5309–5312.
- 103 K. Li, X. Shao, L. Tseng and S. J. Malcolmson, *J. Am. Chem. Soc.*, 2018, **140**, 598–601.
- 104 X. Shao, K. Li and S. J. Malcolmson, *J. Am. Chem. Soc.*, 2018, **140**, 7083–7087.
- 105 P. Zhou, X. Shao and S. J. Malcolmson, *J. Am. Chem. Soc.*, 2021, **143**, 13999–14008.
- 106 J. L. Schwarz, F. Schäfers, A. Tlahuext-Aca, L. Lückemeier and F. Glorius, *J. Am. Chem. Soc.*, 2018, **140**, 12705–12709.
- 107 F. Schäfers, S. Dutta, R. Kleinmans, C. Mück-Lichtenfeld and F. Glorius, *ACS Catal.*, 2022, **12**, 12281–12290.
- 108 Y. C. Hee and J. P. Morken, *J. Am. Chem. Soc.*, 2008, **130**, 16140–16141.
- 109 H. Y. Cho, Z. Yu and J. P. Morken, *Org. Lett.*, 2011, **13**, 5267–5269.
- 110 D. Hemming, R. Fritzemeier, S. A. Westcott, W. L. Santos and P. G. Steel, *Chem. Soc. Rev.*, 2018, **47**, 7477–7494.
- 111 F. Meng, H. Jang, B. Jung and A. H. Hoveyda, *Angew. Chem., Int. Ed.*, 2013, **52**, 5046–5051.
- 112 K. Yeung, R. E. Ruscoe, J. Rae, A. P. Pulis and D. J. Procter, *Angew. Chem., Int. Ed.*, 2016, **55**, 11912–11916.
- 113 J. Chen, S. Gao, J. D. Gorden and M. Chen, *Org. Lett.*, 2019, **21**, 4638–4641.
- 114 T. Miura, J. Nakahashi, T. Sasatsu and M. Murakami, *Angew. Chem., Int. Ed.*, 2019, **58**, 1138–1142.
- 115 M. J. Hesse, S. Essafi, C. G. Watson, J. N. Harvey, D. Hirst, C. L. Willis and V. K. Aggarwal, *Angew. Chem., Int. Ed.*, 2014, **53**, 6145–6149.
- 116 B. M. Trost, J. J. Cregg and N. Quach, *J. Am. Chem. Soc.*, 2017, **139**, 5133–5139.

